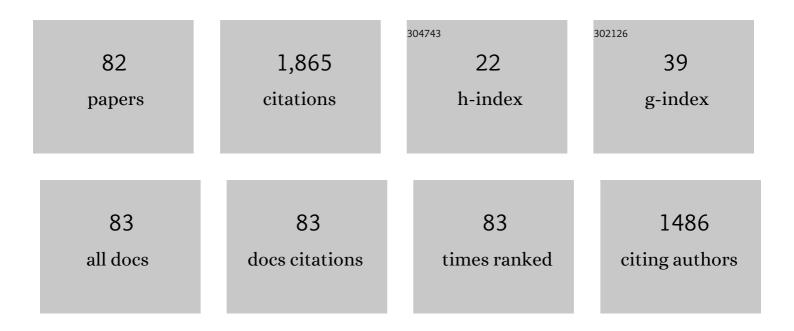


List of Publications by Year in descending order

Source: https://exaly.com/author-pdf/1713426/publications.pdf Version: 2024-02-01



YU CAO

#	Article	IF	CITATIONS
1	Overview of first Wendelstein 7-X high-performance operation. Nuclear Fusion, 2019, 59, 112004.	3.5	165
2	Overview of the JET results in support to ITER. Nuclear Fusion, 2017, 57, 102001.	3.5	150
3	Major results from the first plasma campaign of the Wendelstein 7-X stellarator. Nuclear Fusion, 2017, 57, 102020.	3.5	128
4	Magnetic configuration effects on the Wendelstein 7-X stellarator. Nature Physics, 2018, 14, 855-860.	16.7	110
5	Performance of Wendelstein 7-X stellarator plasmas during the first divertor operation phase. Physics of Plasmas, 2019, 26, .	1.9	83
6	First results from divertor operation in Wendelstein 7-X. Plasma Physics and Controlled Fusion, 2019, 61, 014035.	2.1	75
7	Efficient generation of energetic ions in multi-ion plasmas by radio-frequency heating. Nature Physics, 2017, 13, 973-978.	16.7	73
8	Demonstration of reduced neoclassical energy transport in Wendelstein 7-X. Nature, 2021, 596, 221-226.	27.8	69
9	Infrared imaging systems for wall protection in the W7-X stellarator (invited). Review of Scientific Instruments, 2018, 89, 10E116.	1.3	58
10	Q-Band X-Mode Reflectometry and Density Profile Reconstruction. Plasma Science and Technology, 2015, 17, 985-990.	1.5	53
11	Overview of ASDEX Upgrade results. Nuclear Fusion, 2017, 57, 102015.	3.5	53
12	Electron-cyclotron-resonance heating in Wendelstein 7-X: A versatile heating and current-drive method and a tool for in-depth physics studies. Plasma Physics and Controlled Fusion, 2019, 61, 014037.	2.1	43
13	Drift effects on W7-X divertor heat and particle fluxes. Plasma Physics and Controlled Fusion, 2019, 61, 125001.	2.1	35
14	First divertor physics studies in Wendelstein 7-X. Nuclear Fusion, 2019, 59, 096014.	3.5	34
15	First Observation of a Stable Highly Dissipative Divertor Plasma Regime on the Wendelstein 7-X Stellarator. Physical Review Letters, 2019, 123, 025002.	7.8	33
16	Characterization of the W7-X scrape-off layer using reciprocating probes. Nuclear Fusion, 2019, 59, 086013.	3.5	32
17	Understanding detachment of the W7-X island divertor. Nuclear Fusion, 2021, 61, 086012.	3.5	29
18	Characterisation of the deuterium recycling at the W divertor target plates in JET during steady-state plasma conditions and ELMs. Physica Scripta, 2016, T167, 014076.	2.5	27

#	Article	IF	CITATIONS
19	Effects of toroidal plasma current on divertor power depositions on Wendelstein 7-X. Nuclear Fusion, 2019, 59, 106015.	3.5	26
20	Methods for quantitative study of divertor heat loads on W7-X. Nuclear Fusion, 2019, 59, 066007.	3.5	26
21	Overview of the results from divertor experiments with attached and detached plasmas at Wendelstein 7-X and their implications for steady-state operation. Nuclear Fusion, 2021, 61, 106003.	3.5	24
22	Experimental confirmation of efficient island divertor operation and successful neoclassical transport optimization in Wendelstein 7-X. Nuclear Fusion, 2022, 62, 042022.	3.5	24
23	Overview of progress in European medium sized tokamaks towards an integrated plasma-edge/wall solution ^a . Nuclear Fusion, 2017, 57, 102014.	3.5	23
24	First demonstration of radiative power exhaust with impurity seeding in the island divertor at Wendelstein 7-X. Nuclear Fusion, 2019, 59, 106020.	3.5	23
25	Measurement of the plasma edge profiles using the combined probe on W7-X. Nuclear Fusion, 2017, 57, 126020.	3.5	22
26	Material erosion and deposition on the divertor of W7-X. Physica Scripta, 2020, T171, 014035.	2.5	20
27	Diagnostic set-up and modelling for investigation of synergy between 3D edge physics and plasma-wall interactions on Wendelstein 7-X. Nuclear Fusion, 2017, 57, 066049.	3.5	18
28	Stable heat and particle flux detachment with efficient particle exhaust in the island divertor of Wendelstein 7-X. Nuclear Fusion, 0, , .	3.5	18
29	First three-dimensional edge plasma transport simulations with magnetic perturbations induced by lower hybrid waves on EAST. Nuclear Fusion, 2018, 58, 106008.	3.5	16
30	Tuning of the rotational transform in Wendelstein 7-X. Nuclear Fusion, 2019, 59, 126004.	3.5	16
31	Edge plasma measurements on the OP 1.2a divertor plasmas at W7-X using the combined probe. Nuclear Materials and Energy, 2019, 19, 179-183.	1.3	15
32	Validation of the BEAMS3D neutral beam deposition model on Wendelstein 7-X. Nuclear Fusion, 2020, 60, 076020.	3.5	15
33	Characterization of the radial electric field and edge velocity shear in Wendelstein 7-X. Nuclear Fusion, 2020, 60, 106019.	3.5	14
34	Quantification of erosion pattern using picosecond-LIBS on a vertical divertor target element exposed in W7-X. Nuclear Fusion, 2021, 61, 016025.	3.5	14
35	<i>Ex situ</i> analysis of W7-X divertor plasma-facing components by picosecond laser diagnostics. Physica Scripta, 2020, T171, 014018.	2.5	13
36	EMC3-EIRENE simulation of first wall recycling fluxes in W7-X with relation to H-alpha measurements. Plasma Physics and Controlled Fusion, 2021, 63, 045016.	2.1	13

#	Article	IF	CITATIONS
37	First neutral beam experiments on Wendelstein 7-X. Nuclear Fusion, 2021, 61, 096008.	3.5	13
38	Validating the ASCOT modelling of NBI fast ions in Wendelstein 7-X stellarator. Journal of Instrumentation, 2019, 14, C10012-C10012.	1.2	12
39	Armoring of the Wendelstein 7-X divertor-observation immersion-tubes based on NBI fast-ion simulations. Fusion Engineering and Design, 2019, 146, 862-865.	1.9	12
40	Plasma–surface interaction in the stellarator W7-X: conclusions drawn from operation with graphite plasma-facing components. Nuclear Fusion, 2022, 62, 016006.	3.5	12
41	Radial and poloidal correlation reflectometry on Experimental Advanced Superconducting Tokamak. Review of Scientific Instruments, 2015, 86, 083503.	1.3	11
42	Effect of toroidal plasma currents on the Wendelstein 7-X Scrape-Off Layer. Plasma Physics and Controlled Fusion, 2019, 61, 125014.	2.1	11
43	Wendelstein 7-X on the path to long-pulse high-performance operation. Fusion Engineering and Design, 2021, 167, 112381.	1.9	10
44	Plasma-wall interaction studies in W7-X: main results from the recent divertor operations. Physica Scripta, 2021, 96, 124059.	2.5	10
45	The effects of magnetic topology on the scrape-off layer turbulence transport in the first divertor plasma operation of Wendelstein 7-X using a new combined probe. Nuclear Fusion, 2019, 59, 066001.	3.5	9
46	Observation of thermal events on the plasma facing components of Wendelstein 7-X. Journal of Instrumentation, 2019, 14, C11002-C11002.	1.2	9
47	Understanding baffle overloads observed in high-mirror configuration on Wendelstein 7-X. Nuclear Fusion, 2020, 60, 096012.	3.5	9
48	Multi-channel poloidal correlation reflectometry on experimental advanced superconducting tokamak. Review of Scientific Instruments, 2016, 87, 11E707.	1.3	8
49	Validating fast-ion wall-load IR analysis-methods against W7-X NBI empty-torus experiment. Journal of Instrumentation, 2019, 14, P07018-P07018.	1.2	8
50	Large wetted areas of divertor power loads at Wendelstein 7-X. Nuclear Fusion, 2020, 60, 084003.	3.5	8
51	Bolometer tomography on Wendelstein 7-X for study of radiation asymmetry. Nuclear Fusion, 2021, 61, 116043.	3.5	8
52	Integrated modelling: Coupling of surface evolution and plasma-impurity transport. Nuclear Materials and Energy, 2020, 25, 100821.	1.3	7
53	Hydrogen content in divertor baffle tiles in Wendelstein 7-X. Nuclear Materials and Energy, 2021, 26, 100943.	1.3	7
54	Model for current drive induced crash cycles in W7-X. Nuclear Fusion, 2021, 61, 126040.	3.5	7

#	Article	IF	CITATIONS
55	Evaluation of NVIDIA Xavier NX Platform for Real-Time Image Processing for Plasma Diagnostics. Energies, 2022, 15, 2088.	3.1	7
56	Impact of the JET ITER-like wall on H-mode plasma fueling. Nuclear Fusion, 2017, 57, 066024.	3.5	6
57	Observations of the effects of magnetic topology on the SOL characteristics of an electromagnetic coherent mode in the first experimental campaign of W7-X. Nuclear Fusion, 2018, 58, 046002.	3.5	6
58	Measurement and modeling of magnetic configurations to mimic overload scenarios in the W7-X stellarator. Nuclear Fusion, 2019, 59, 066041.	3.5	6
59	Initial results from the hotspot detection scheme for protection of plasma facing components in Wendelstein 7-X. Nuclear Materials and Energy, 2019, 19, 335-339.	1.3	6
60	Characteristics of the SOL turbulence structure in the first experimental campaign on W7-X with limiter configuration. Physics of Plasmas, 2018, 25, .	1.9	5
61	Impact of n  =  1 field on the non-axisymmetric magnetic perturbations associated with the ed mode crashes in the ASDEX Upgrade tokamak. Nuclear Fusion, 2019, 59, 054002.	$ge_{3.5}^{localize}$	ed 5
62	The evolution of the bound particle reservoir in Wendelstein 7-X and its influence on plasma control. Nuclear Fusion, 2021, 61, 036031.	3.5	5
63	2D measurements of parallel counter-streaming flows in the W7-X scrape-off layer for attached and detached plasmas. Nuclear Fusion, 2021, 61, 116039.	3.5	5
64	Plasma radiation behavior approaching high-radiation scenarios in W7-X. Nuclear Fusion, 2021, 61, 126002.	3.5	5
65	Analysis of hydrogen fueling, recycling, and confinement at Wendelstein 7-X via a single-reservoir particle balance. Nuclear Fusion, 2022, 62, 036023.	3.5	5
66	Study of Striated Heat Flux on EAST Divertor Plates Induced by LHW Using Infrared Camera. Plasma Science and Technology, 2014, 16, 93-98.	1.5	4
67	Magnetic configuration effects on the edge heat flux in the limiter plasma on W7-X measured using the infrared camera and the combined probe. Plasma Science and Technology, 2018, 20, 054003.	1.5	4
68	Tools for Image Analysis and First Wall Protection at W7-X. Fusion Science and Technology, 2020, 76, 933-941.	1.1	4
69	First attempt to quantify W7-X island divertor plasma by local experiment-model comparison. Nuclear Fusion, 2021, 61, 106018.	3.5	4
70	Validation of theory-based models for the control of plasma currents in W7-X divertor plasmas. Nuclear Fusion, 2021, 61, 126022.	3.5	4
71	Real-Time Detection of Overloads on the Plasma-Facing Components of Wendelstein 7-X. Applied Sciences (Switzerland), 2021, 11, 11969.	2.5	4
72	2D coherence imaging measurements of C ²⁺ ion temperatures in the divertor of Wendelstein 7-X. Nuclear Fusion, 2021, 61, 106041.	3.5	3

#	ARTICLE	IF	CITATIONS
73	Confinement degradation and plasma loss induced by strong sawtooth crashes at W7-X. Nuclear Fusion, 2021, 61, 116053.	3.5	3
74	Learning control coil currents from heat-flux images using convolutional neural networks at Wendelstein 7-X. Plasma Physics and Controlled Fusion, 2021, 63, 025009.	2.1	3
75	Plasma beta effects on the edge magnetic field structure and divertor heat-loads in Wendelstein 7-X high-performance scenarios. Nuclear Fusion, 0, , .	3.5	3
76	Anisotropic diffusion as a proxy model for the estimation of heat-loads on plasma-facing components. Plasma Physics and Controlled Fusion, 0, , .	2.1	3
77	Endoscopes for observation of plasma-wall interactions in the divertor of Wendelstein 7-X. Fusion Engineering and Design, 2019, 146, 19-22.	1.9	1
78	Combining research with safety: Performance of the Wendelstein 7-X video diagnostic system. Fusion Engineering and Design, 2019, 146, 874-877.	1.9	1
79	Approaches for quantitative study of divertor heat loads on W7-X. , 0, , .		1
80	Parametrisation of target heat flux distribution and study of transport parameters for boundary modelling in W7-X. Nuclear Fusion, 0, , .	3.5	1
81	Characteristics of pre-ELM structures during ELM control experiment on JET withn  =  2 magnet perturbations. Nuclear Fusion, 2016, 56, 092011.	ic _{3.5}	0
82	Thermographic reconstruction of heat load on the first wall of Wendelstein 7-X due to ECRH shine-through power. Nuclear Fusion, 2021, 61, 066002.	3.5	0